MATHEMATICAL BIOSCIENCES
AND ENGINEERING
Volume **12**, Number **1**, February **2015**

doi:10.3934/mbe.2015.12.209

pp. **209–231**

AGGREGATION AND ENVIRONMENTAL TRANSMISSION IN CHRONIC WASTING DISEASE

Olga Vasilyeva

Department of Mathematics, Christopher Newport University
1 Avenue of the Arts
Newport News, VA 23606, USA

Tamer Oraby

Department of Mathematics, The University of Texas-Pan American
1201 W. University Drive
Edinburg, TX 78539, USA

Frithjof Lutscher

Department of Mathematics, Univeristy of Ottawa
585 King Edward
Ottawa, ON K1N 6N5 , Canada

(Communicated by James Watmough)

Abstract. Disease transmission depends on the interplay between the infectious agent and the behavior of the host. Some diseases, such as Chronic Wasting Disease, can be transmitted directly between hosts as well as indirectly via the environment. The social behavior of hosts affects both of these pathways, and a successful intervention requires knowledge of the relative influence of the different etiological and behavioral aspects of the disease. We develop a strategic differential equation model for Chronic Wasting Disease and include direct and indirect transmission as well as host aggregation into our model. We calculate the basic reproduction number and perform a sensitivity analysis based on Latin hypercube sampling from published parameter values. We find conditions for the existence of an endemic equilibrium, and show that, under a certain mild assumption on parameters, the model does not exhibit a backward bifurcation or bistability. Hence, the basic reproduction number constitutes the disease elimination threshold. We find that the prevalence of the disease decreases with host aggregation and increases with the lifespan of the infectious agent in the environment.

1. **Introduction.** Discovered in North America in 1960s, Chronic Wasting Disease (CWD) affects species of the deer family. CWD is caused by accumulation of the pathogen (misfolded prions) in the animal's lymphoid tissue and central nervous system, and leads to extensive tissue damage and eventual death of the host [1, 6, 24]. Several mathematical models have been proposed to study the dynamics of CWD and find control strategies, e.g. [2, 19, 18, 23].

2010 *Mathematics Subject Classification.* Primary: 92D30.

Key words and phrases. Chronic wasting disease, environmental transmission, aggregation, disease free equilibrium, endemic equilibrium.

One of the most important characteristics of any disease is the way by which it is transmitted from infected to susceptible individuals. One distinguishes direct (via actual contact) and indirect (via contaminated environment) transmission. Many previous approaches to modeling of CWD focused on direct transmission only [13, 21, 23]. As pointed out in [2], the control measures based on such approaches (such as culling to reduce deer density) were not successful in reducing CWD prevalence [8]. Numerous studies show that indirect transmission plays a significant role in CWD dynamics [2, 19, 16]. Prions may attach to soil particles and remain contagious for at least two years [7]. As a result, environmental persistence of prions becomes a secondary source of infection, even after the infectious animal's death.

Models that incorporate and compare both transmission modes are typically high-dimensional simulation models [2]. The first goal of this paper is to develop and analyze the relative importance of direct and indirect transmission in an analytically tractable strategic model.

Transmission pathways of CWD, and many other wildlife infectious diseases, typically depend on the social structure and interaction of the affected population. The importance of animals' (and environmental prions') aggregation in modeling of CWD was first recognized in [2], where the authors performed extensive numerical simulations of a high-dimensional CWD model with direct and indirect transmission. The second goal of this paper is to incorporate aggregation into the simpler strategic model and evaluate its importance for disease establishment and prevalence.

We introduce our model in Section 2, and show that solutions remain bounded and non-negative with respect to the flow corresponding to the model. In Section 3, we analyze stability of the zero state and the disease-free equilibrium (DFE). We also derive and analyze the formula for the basic reproduction number R_0. In Section 4, we investigate the question of existence of an endemic equilibrium (EE) in the case of low aggregation, and give a sufficient condition of existence and uniqueness of EE in this case. In Section 5, we use center manifold theory combined with numerical tools to establish that for all aggregation levels, the DFE loses stability at $R_0 = 1$ in a forward bifurcation, with an EE appearing when $R_0 > 1$. This is done under a mild technical assumption, which according to numerics, always holds for our parameter ranges. In Section 6, we perform numerical simulations and sensitivity analysis of our model based on partial rank correlation coefficients and Latin hypercube sampling. We end with a discussion of the biological implications of our results and directions for further research.

2. **Derivation of the model.** We derive our strategic model to assess the effects of transmission pathways and aggregation on the dynamics of CWD. For the simplest possible set-up, we choose only the three compartments of susceptible (S) and infectious (I) individuals and the amount of prions in the environment (V). The dynamics of these compartments are given by the population dynamics of deer, the disease transmission and the production and decay of prions by the following system of differential equations

$$\begin{aligned}
\frac{dS}{dt} &= \frac{r(S+(1-\alpha)I)}{1+\delta N} - \mu S - S\,\mathbb{F}_d - S\,\mathbb{F}_e \\
\frac{dI}{dt} &= \frac{\alpha r I}{1+\delta N} - (\mu+\nu)I + S\,\mathbb{F}_d + S\,\mathbb{F}_e \\
\frac{dV}{dt} &= -\tau V + \epsilon I,
\end{aligned} \tag{1}$$

where $N = S + I$ is the total deer population.

The per capita birth rate is modeled by the Beverton-Holt function $\frac{r}{1+\delta N}$, where r denotes the maximal birth rate and δ the strength of intraspecific competition [20, 22]. Parameter $0 \leq \alpha \leq 1$ is the probability of vertical disease transmission. When $\alpha = 0$, all deer are born susceptible; when $\alpha = 1$, offspring are in the same class as their parents. The death rate due to natural causes is denoted by μ. The additional death rate ν of infected individuals accounts for disease-induced deaths. If we consider harvesting as a control strategy, then μ is the sum of natural death and unspecific harvesting; ν is disease-induced death plus specific harvesting (if the latter is possible at all). Prions in the environment decay exponentially with rate τ, and are shed by the infectious animals with rate ε.

The terms $S\,\mathbb{F}_d$ and $S\,\mathbb{F}_e$ describe direct and environmental disease transmission, respectively. The respective force of infection, $\mathbb{F}_d$ and $\mathbb{F}_e$, give the per-capita rate of infection. We choose these terms very general to allow for greatest flexibility in our model. We begin with a detailed derivation of these terms that specify our assumptions and define our parameters.

To derive the direct transmission rate, $\mathbb{F}_d$, let the random variable X be the number of contacts that a single animal makes per unit time. Assuming homogeneous mixing of individuals, the probability that any single contact is with an infected animal is given by the prevalence, $\frac{I}{N}$. We denote by p_d the probability that a contact with an infectious animal leads to transmission of infection. Then the probability of a single contact between a susceptible individual and another animal resulting in a disease transmission is $p_d\,\frac{I}{N}$. The probability that at least one of m contacts leads to transmission is

$$P(\text{transmission}|X = m) = 1 - \left(1 - p_d \frac{I}{N}\right)^m. \tag{2}$$

This formula is also valid for $m = 0$, as the probability of infection is 0.

The probability of direct disease transmission (per individual, per unit time) is given by

$$\begin{aligned}
\mathbb{P}_d &= \sum_{m=0}^{\infty} P\left(\text{transmission } |X = m\right) P\left(X = m\right) \\
&= \sum_{m=0}^{\infty} \left(1 - \left(1 - p_d \frac{I}{N}\right)^m\right) P\left(X = m\right) \\
&= E\left(1 - \left(1 - p_d \frac{I}{N}\right)^X\right) = 1 - E\left(e^{X \ln\left(1 - p_d \frac{I}{N}\right)}\right) \\
&= 1 - M_X\left(\ln\left(1 - p_d \frac{I}{N}\right)\right).
\end{aligned}$$

Here, $E(Y)$ is the expected value of a random variable Y, and M_X is the moment generating function of the random variable X. M_X exists at $\ln\left(1 - p_d \frac{I}{N}\right)$, since this expression is negative and X is always non-negative.

We now assume that the number of contacts follows a Pólya distribution (a generalization of the Negative Binomial distribution) with mean $\lambda_d \in [0, \infty)$ and aggregation (clumping) parameter $k_d \in [0, \infty)$ [17, 2]. Thus, $X \sim$ Pólya$(k_d, \tilde{p})$, where $\lambda_d = k_d \frac{\tilde{p}}{1-\tilde{p}}$, so that k_d and λ_d have the same units and $\tilde{p}$ is a probability. Smaller values of k_d (higher aggregation) imply higher likelihood of consecutive

contacts between two individuals, and this positive correlation between two consecutive contacts implies higher variance of X. This contact pattern can be explained by grouping and kinship as well as frequent visits to the same locations. In social groups this pattern maybe more realistic than the Poisson contact pattern of uncorrelated contacts between individuals.

Substituting the formula for the moment-generating function of the Pólya (Negative Binomial) distribution, we obtain

$$M_X(s) = \left(\frac{1-\tilde{p}}{1-\tilde{p}e^s}\right)^{k_d} = \left(\frac{1}{1+\frac{\lambda_d}{k_d}-\frac{\lambda_d e^s}{k_d}}\right)^{k_d}. \tag{3}$$

Thus, the probability of an infection during $[t, t+\triangle t)$ is

$$\begin{aligned}\mathbb{P}_d(\triangle t) =& 1 - M_X\left(\ln\left(1-p_d\frac{I}{N}\right)\right) = 1-\left(\frac{1}{1+\frac{\lambda_d\triangle t}{k_d\triangle t}-\frac{\lambda_d\triangle t}{k_d\triangle t}\left(1-p_d\frac{I}{N}\right)}\right)^{k_d\triangle t}\\ =& 1-\left(1+p_d\frac{\lambda_d}{k_d}\frac{I}{N}\right)^{-k_d\triangle t} = 1-e^{-k_d\triangle t\,\ln\left(1+p_d\frac{\lambda_d}{k_d}\frac{I}{N}\right)}\end{aligned}$$

The force of infection is then the derivative of $\mathbb{P}_d$ evaluated at $\triangle t = 0$, which is

$$\mathbb{F}_d = \mathbb{P}_d'(0) = k_d \ln\left(1+p_d\frac{\lambda_d}{k_d}\frac{I}{N}\right). \tag{4}$$

Remark 1. When aggregation is small, the value of k_d is high, and the Negative Binomial distribution can be approximated by the Poisson distribution with the same mean λ_d. In this case we obtain the simpler expression, $\mathbb{F}_d = \lambda_d p_d \frac{I}{N}$.

Finally, we consider how the expected number of contacts $E(X) = \lambda_d$ depends on population density. The two standard cases $\lambda_d(N) = \bar{\lambda}_d$ and $\lambda_d(N) = \bar{\lambda}_d N$ lead to the so-called frequency and density dependent case, respectively. There is some controversy about which of these choices is more appropriate for wildlife diseases [3, 15], experimental data for CWD is ambivalent in this regard [23].

Some authors have used certain interpolations between the two forms, for example

Case 1 [14]: $\lambda_d(N) = \bar{\lambda}_d\left(\frac{N}{K}\right)^{1-q}$, where $0 \le q \le 1$ and $\bar{\lambda}_d$ is a constant.

Case 2 [2]: $\lambda_d(N) = \frac{\bar{\lambda}_d N}{1-\theta+\theta\frac{N}{K}}$, where $0 \le \theta \le 1$ and $\bar{\lambda}_d$ is a constant.

Case 3 [9]: $\lambda_d(N) = \frac{\gamma N}{1+\frac{\gamma}{\bar{\lambda}_d}N}$, where $\gamma, \bar{\lambda}_d$ are constants.

Here K is a scale parameter, having the same dimension as N. The first two cases, while interpolating between density dependent ($q = \theta = 0$) and frequency dependent ($q = \theta = 1$), suffer from a number of drawbacks [9]. Case 3 is inspired by the mechanistic underpinning of Holling's disc equation; it is essentially density dependent when N is small and frequency dependent when N is large.

The approach in Case 3 (saturating incidence) has been used to describe environmental transmission in [10].

We apply the same considerations as above to model the environmental transmission process. We denote by D the total amount of "deposits" in the environment, i.e. animal waste, carcasses, etc. Then V/D is equivalent to the term I/N for direct transmission. We denote by p_e the probability that a contact with contaminated deposit leads to disease transmission, by k_e the aggregation of contacts with deposits, and by λ_e the rate of contact with deposits in the environment. We assume

that $\lambda_e = \bar{\lambda}_e D$ is proportional to D and independent of N. These considerations lead to an expression similar to (4) with I/N replaced by V/D. Instead, we consider the slightly more general case

$$\mathbb{F}_e = k_e \ln\left(1 + \bar{\lambda}_e \frac{p_e V}{k_e(1+\sigma V)}\right). \tag{5}$$

When $\sigma = 0$, we have the exact same scenario as for direct transmission. However, some empirical results indicate that the presence and not so much the quantity of prions in the environment determines infection [12]. Hence, the rate of disease transmission could somehow saturate when prions are abundant. This effect is heuristically modeled by $\sigma > 0$. A similar form, in the limit as $k_e \to \infty$ has recently been used for environmental transmission modeling [4].

In summary, model (1) with transmission terms (4) and (5) reads

$$\begin{aligned}
\frac{dS}{dt} &= \frac{r(S+(1-\alpha)I)}{1+\delta N} - \mu S - S k_d \ln\left(1+\lambda_d(N)\frac{p_d I}{N k_d}\right) - S k_e \ln\left(1+\frac{\lambda_e p_e V}{k_e(1+\sigma V)}\right)\\
\frac{dI}{dt} &= \frac{\alpha r I}{1+\delta N} - (\mu+\nu) I + S k_d \ln\left(1+\lambda_d(N)\frac{p_d I}{N k_d}\right) + S k_e \ln\left(1+\frac{\lambda_e p_e V}{k_e(1+\sigma V)}\right)\\
\frac{dV}{dt} &= -\tau V + \epsilon I.
\end{aligned} \tag{6}$$

Since no confusion can arise, we simplified notation by writing λ_e instead of $\bar{\lambda}_e$. For a summary of variables and parameters, please see Table 1.

We finish this section by showing that system (6) has bounded solutions and that the set $(\mathbb{R}^+)^3$ is positively invariant with respect to the flow of (6).

We prove positive invariance first.

Proposition 1. *Suppose $(S(t), I(t), V(t))$ is a solution of (6) such that $S(0) > 0$, $I(0) > 0$ and $V(0) > 0$. Then $S(t) > 0$, $I(t) > 0$ and $V(t) > 0$ for all $t \geq 0$ for which the solution exists.*

Proof. Suppose at least one of S, I or V takes a value ≤ 0. Let $t_0 > 0$ be smallest such that at least one of S, I or V takes values 0 at t_0.

Case 1. Suppose $S(t_0) = 0$. Since $S(t) > 0$ for $0 < t < t_0$, we have $S'(t_0) \leq 0$. Then we claim that $I(t_0) = 0$. Otherwise, $I(t_0) > 0$, and from the first equation of (6), we get $S'(t_0) > 0$, a contradiction. Since $S(t_0) = 0$ and $I(t_0) = 0$, then, by the Existence-Uniqueness Theorem, $(S(t), I(t), V(t)) = (0, 0, V(t_0)e^{-\tau(t-t_0)})$ on some neighborhood of t_0, contradicting the assumption $S(t) > 0$, $I(t) > 0$ for $0 < t < t_0$. Thus, $S(t_0) > 0$.

Case 2. Suppose $I(t_0) = 0$. Since $I(t) > 0$ for $0 < t < t_0$, we have $I'(t_0) \leq 0$. We already know from Case 1, that $S(t_0) > 0$. From the second equation of (6), we conclude that $V(t_0) = 0$. Otherwise, $V(t_0) > 0$ and, hence, $I'(t_0) > 0$, a contradiction. Thus, $(S(t_0), I(t_0), V(t_0)) = (S(t_0), 0, 0)$. But (6) has a solution of the form $(\varphi(t), 0, 0)$, where $\varphi(t)$ is the solution of

$$\frac{dS}{dt} = \frac{rS}{1+\delta S} - \mu S,$$

with $\varphi(t_0) = S(t_0)$. By the Existence-Uniqueness Theorem, $(S(t), I(t), V(t)) = (\varphi(t), 0, 0)$ on some neighborhood of t_0, contradicting the assumption $S(t) > 0$, $I(t) > 0$ for $0 < t < t_0$. Thus, $I(t_0) > 0$.

Case 3. Suppose $V(t_0) = 0$. Since $V(t) > 0$ for $0 < t < t_0$, we have $V'(t_0) \leq 0$. Then from the third equation of (6), we conclude that $I(t_0) = 0$, a contradiction with Case 2. Thus, $V(t_0) > 0$.

We conclude that $S(t), I(t), V(t) > 0$ for all $t \geq 0$. □

Next, we will use the above proposition to show that the set

$$\{(S, I, V) : S, I, V \geq 0\} \subset \mathbb{R}^3$$

is also positively invariant with respect to the flow of (6).

Proposition 2. *Suppose $(S(t), I(t), V(t))$ is a solution of (6) such that $S(0) \geq 0$, $I(0) \geq 0$ and $V(0) \geq 0$. Then $S(t) \geq 0$, $I(t) \geq 0$ and $V(t) \geq 0$ for all $t \geq 0$ for which the solution exists.*

Proof. Cases when $S(0), I(0), V(0)$ are all zero or all positive are clear.

Suppose $S(0) > 0, I(0) = V(0) = 0$. By uniqueness, the solution is given by $(S(t), 0, 0)$ where $S(t)$ satisfies the differential equation

$$\frac{dS}{dt} = \frac{rS}{1 + \delta S} - \mu S.$$

Since the above equation has a trivial solution, we have $S(t) > 0$ for all $t \geq 0$. The case when $S(0) = 0, I(0) = 0$ and $V(0) > 0$ is done similarly.

Next, suppose $S(0) > 0, I(0) > 0, V(0) = 0$. In this case, $V'(0) > 0$. Thus for sufficiently small $t > 0$, we have $V(t) > 0$, as well as $S(t) > 0$ and $I(t) > 0$. By Proposition 1, $S(t), I(t), v(t) > 0$ for all $t > 0$. Similar argument proves the case when $S(0) > 0, I(0) = 0, V(0) > 0$.

Now, let $S(0) = 0, I(0) > 0, V(0) > 0$. If $\alpha < 1$, we have $S'(0) > 0$. Thus for sufficiently small $t > 0$, we have $S(t) > 0$, as well as $I(t) > 0$ and $V(t) > 0$. By Proposition 1, $S(t), I(t), V(t) > 0$ for all $t > 0$. If $\alpha = 1$, then the solution will be of the form $(0, I(t), V(t))$, where $I(t)$ satisfies

$$\frac{dI}{dt} = \frac{\alpha r I}{1 + \delta I} - (\mu + \nu) I,$$

and $V(t)$ satisfies

$$\frac{dV}{dt} = -\tau V + \epsilon I.$$

Thus, we solve for $I(t)$ and note that $I(t) > 0$ for all $t \geq 0$ (since the equation has trivial solution $I \equiv 0$). Substituting $I(t)$ into the equation for V, we also get $V(t) > 0$ for all $t \geq 0$. The only remaining case when $S(0) = 0, I(0) > 0, V(0) = 0$ is similar. □

Lemma 2.1. *Let $f(t)$ be a differentiable function, such that*

$$f'(t) \leq \alpha - \beta f(t),$$

for any $t \geq 0$, and $f(0) \geq 0$, where $\alpha, \beta > 0$ are some constants. Then $f(t) \leq \max(f(0), \frac{\alpha}{\beta})$ for any $t \geq 0$.

Proof. The function f is bounded by the solution of the differential equation that results from replacing $\leq$ with $=$. This solution is monotone since the equation is one-dimensional. The steady state is α/β. If $f(0) < \alpha/\beta$ then $f(t) < \alpha/\beta$ for all times. If $f(0) > \alpha/\beta$ then $f' < 0$ for all times. □

We are now ready to prove boundedness of solutions of (6).

variable/ parameter	description	unit
S	susceptible population	$\#$
I	infected population	$\#$
V	contaminated deposits	$\diamondsuit$
r	(intrinsic) growth rate	$\frac{1}{t}$
μ	natural death rate (plus harvesting, if any)	$\frac{1}{t}$
α	hereditary infection factor	-
δ	logistic growth coefficient	$\frac{1}{\#}$
λ_d	direct contacts per animal	$\frac{1}{t}$
p_d	probability of successful direct transmission	-
k_d	aggregation of direct contacts	$\frac{1}{t}$
λ_e	indirect contacts per animal	$\frac{1}{t}$
p_e	probability of successful indirect transmission	-
k_e	aggregation of indirect contacts	$\frac{1}{t}$
ν	death rate due to disease (+ specific harvesting, if any)	$\frac{1}{t}$
σ	prion saturation constant	$\frac{1}{\diamondsuit}$
τ	prion decay rate	$\frac{1}{t}$
ε	prion shedding rate	$\frac{\diamondsuit}{\#t}$

TABLE 1. This table gives the description and units of the variables and parameters used in our system. Here, $\#$ denotes the unit used for the population size (e.g. thousands of deer), and $\diamondsuit$ denotes the unit of the amount of contaminated deposits in the environment. We denote the time unit by t. Dimensionless parameters are denoted by -.

Proposition 3. *Suppose $(S(t), I(t), V(t))$ is a solution of (6) with $S(0), I(0), V(0) \geq 0$. Then there exists $C > 0$ such that $S(t), I(t), V(t) \in [0, C]$ for all $t \geq 0$ for which the solution exists.*

Proof. Recall that $N(t) = S(t) + I(t)$. Adding the first two equations of (6), we get

$$\frac{dN}{dt} = \frac{rN}{1 + \delta N} - \mu N - \nu I.$$

Since $N(t), I(t) \geq 0$ for all $t \geq 0$ and , we have

$$N'(t) \leq \frac{r}{\delta} - \mu N(t),$$

for all $t \geq 0$. By Lemma 2.1, $N(t) \leq \bar{N} = \max(N(0), \frac{r}{\delta\mu})$ for all $t \geq 0$. In particular, $S(t), I(t) \leq \bar{N}$ for all $t \geq 0$.

Then the third equation of (6) implies

$$V'(t) \leq \varepsilon \bar{N} - \tau V(t),$$

for all $t \geq 0$. Thus, $V(t) \leq \bar{V} = \max(V(0), \frac{\varepsilon \bar{N}}{\tau})$, for all $t \geq 0$.

Thus, we can take $C = \max(\bar{N}, \bar{V})$. □

The a-priori estimate in Proposition 3, together with the theorem about extension of solutions of differential equations gives global existence and boundedness of non-negative solutions of (6).

3. **Linearizations about the zero state and the disease-free equilibrium.** Our first goal is to analyze behavior of our model near the trivial steady state. Linearizing (6) at $(0,0,0)$, we obtain the following Jacobi matrix:

$$J(0,0,0) = \begin{pmatrix} r-\mu & r(1-\alpha) & 0 \\ 0 & \alpha r-\mu-\nu & 0 \\ 0 & \varepsilon & -\tau \end{pmatrix}. \tag{7}$$

The equilibrium is (locally asymptotically) stable exactly when all the eigenvalues of J have negative real parts. The eigenvalues of $J(0,0,0)$ are real and are given by

$$\lambda_1 = r-\mu,\ \lambda_2 = \alpha r-\mu-\nu,\ \lambda_3 = -\tau.$$

Note that $\lambda_2 < \lambda_1$ and $\lambda_3 < 0$. Thus, the zero state is locally asymptotically stable exactly when $r < \mu$, i.e. when the death (non-specific harvesting) rate exceeds the growth rate at low densities.

Our next goal is to analyze behavior of the model near its (non-trivial) disease-free equilibrium (DFE) $(S^*,0,0)$. We derive conditions for its stability and obtain a formula for the basic reproduction number, R_0.

Setting I, V and the right-hand sides in our system to zero, we find the steady-state value

$$S^* = \frac{1}{\delta}\left(\frac{r}{\mu}-1\right) = \frac{r-\mu}{\delta\mu}.$$

The value of S^* is positive (i.e. the DFE is biologically relevant) provided the birth rate exceeds the death rate ($r > \mu$).

Next, we linearize our system around $(S^*,0,0)$. The Jacobi matrix is given by

$$J(S^*,0,0) = \begin{pmatrix} -\frac{\mu^2\delta S^*}{r} & \frac{r(1-\alpha)-r\alpha\delta S^*}{(1+\delta S^*)^2} - \lambda_d(S^*)p_d & -S^*\lambda_e p_e \\ 0 & \alpha\mu-\mu-\nu+\lambda_d(S^*)p_d & S^*\lambda_e p_e \\ 0 & \varepsilon & -\tau \end{pmatrix}. \tag{8}$$

Note that one eigenvalue is given by $-\frac{\mu^2\delta S^*}{r} < 0$. The other two are the eigenvalues of the 2×2-matrix

$$\tilde{J} = \begin{pmatrix} \alpha\mu-\mu-\nu+\lambda_d(S^*)p_d & S^*\lambda_e p_e \\ \varepsilon & -\tau \end{pmatrix}.$$

The eigenvalues of $\tilde{J}$ have negative real parts if and only if $\mathrm{tr}(\tilde{J}) < 0$ and $\det(\tilde{J}) > 0$. These conditions give us the following two inequalities:

$$\mu(1-\alpha)+\nu-\lambda_d(S^*)p_d > -\tau \tag{9}$$

$$\mu(1-\alpha)+\nu-\lambda_d(S^*)p_d > \frac{S^*\lambda_e p_e\varepsilon}{\tau}. \tag{10}$$

Since (10) is stronger than (9), we conclude that the disease-free equilibrium is stable if and only if (10) holds.

Following [9], we define the basic reproductive number by

$$R_0 = \frac{\alpha\mu + \frac{S^*\lambda_e p_e\varepsilon}{\tau} + \lambda_d(S^*)p_d}{\mu+\nu}. \tag{11}$$

We interpret the formula for R_0 as follows. The quantity $\dfrac{1}{\mu+\nu}$ represents the average lifespan of an infected individual, while $\frac{1}{\tau}$ can be interpreted as the mean "survival time" of prions in the environment. During one time unit (one year), an infected individual produces, on average, the following amounts of new infections:

$\alpha\mu$ due to vertical transmission (note that the birth rate at the DFE equals μ), $\frac{S^*\lambda_e p_e \varepsilon}{\tau}$ due to indirect contacts, and $\lambda_d(S^*)p_d$ due to direct contacts.

Rewriting the inequality (10) in terms of R_0, we get:

Lemma 3.1. *The DFE is locally asymptotically stable if $R_0 < 1$ and unstable if $R_0 > 1$.*

We illustrate how R_0 depends on model parameters.

First, we note that R_0 is independent of the aggregation parameters k_d and k_e.

Next, we analyze how the basic reproductive number changes when we vary parameters q (Case 1), θ (Case 2) from 0 to 1, or increase S^* (Case 3), i.e. when we change the setting from the density dependent case to the frequency dependent case. The explicit expressions of R_0 are given by

Case 1: $\lambda_d(N) = \bar{\lambda}_d \left(\frac{N}{K}\right)^{1-q}$:

$$R_0 = \frac{\alpha\mu + \frac{S^*\lambda_e p_e \varepsilon}{\tau} + \bar{\lambda}_d p_d \left(\frac{S^*}{K}\right)^{(1-q)}}{\mu + \nu}. \tag{12}$$

Case 2: $\lambda_d(N) = \frac{\bar{\lambda}_d N}{1-\theta+\theta\frac{N}{K}}$:

$$R_0 = \frac{\alpha\mu + \frac{S^*\lambda_e p_e \varepsilon}{\tau} + \frac{\bar{\lambda}_d p_d S^*}{1-\theta+\theta\frac{S^*}{K}}}{\mu + \nu}. \tag{13}$$

Case 3: $\lambda_d(N) = \frac{\gamma N}{1+\frac{\gamma}{\bar{\lambda}_d}N}$:

$$R_0 = \frac{\alpha\mu + \frac{S^*\lambda_e p_e \varepsilon}{\tau} + \frac{\gamma p_d S^*}{1+\frac{\gamma}{\bar{\lambda}_d}S^*}}{\mu + \nu}. \tag{14}$$

Lemma 3.2. *If $S^* > K$, then R_0 is a decreasing function of q (Case 1) or θ (Case 2). If $0 < S^* < K$, then R_0 is an increasing function of q (Case 1) or θ (Case 2). Furthermore, in all the three cases, R_0 is an increasing function of S^*. In Case 3, R_0 is an increasing function of γ.*

Proof. The statement is clear in Case 1. In Case 2, the statement follows from the fact that $\frac{1}{1-\theta+\theta\frac{S^*}{K}}$ is a decreasing function of θ exactly when $S^* > K$. The last statement is straightforward. □

Remark 2. Another way to represent the DFE stability condition is by expressing it as an inequality involving r. Recalling that $S^* = \frac{r-\mu}{\delta\mu}$, we rewrite inequality (10) as

$$r < \mu + \frac{\delta\tau\mu}{\lambda_e p_e \varepsilon}((1-\alpha)\mu + \nu - \lambda_d(S^*)p_d) \tag{15}$$

Thus, in the frequency-dependent case when $\lambda_d(N) = \bar{\lambda}_d$ does not depend on N, we can define the critical growth rate as $r_{cr} = \mu + \frac{\delta\tau\mu}{\lambda_e p_e \varepsilon}((1-\alpha)\mu + \nu - \bar{\lambda}_d p_d)$. In all other cases, we obtain an implicit equation for r, determining stability of the DFE.

4. **Analysis of the endemic equilibrium.** In this section, we present analytical results for the endemic equilibrium (EE), where the disease is present. Since the transmission terms in our model are very general, only some cases can be investigated in detail. We present numerical results and analysis based on center manifold theory, for the general case in Section 5.

We set the right hand sides of (6) equal to zero, and look for a constant solution (S_e, I_e, V_e) where $I_e > 0$. First, note that since $-\tau V_e + \varepsilon I_e = 0$, we get $V_e = \frac{\varepsilon I_e}{\tau}$. The total population at the EE is $N_e = S_e + I_e$. Adding the right hand sides of the first two equations of (21), the transmission terms disappear and we obtain

$$\frac{rN_e}{1+\delta N_e} - \mu N_e - \nu I_e = 0.$$

We can express all steady-state values in terms of N_e, or, more conveniently, in terms of the new variable $x = \frac{r}{1+\delta N_e}$. The expressions are

$$N_e = \frac{r-x}{\delta x} \tag{16}$$

$$I_e = \frac{1}{\nu} N_e (x-\mu) \tag{17}$$

$$S_e = N_e - I_e = \frac{1}{\nu} N_e ((\mu+\nu)-x), \tag{18}$$

$$V_e = \frac{\varepsilon}{\nu\tau} N_e (x-\mu). \tag{19}$$

Setting $x = \mu$, we get the disease free equilibrium (DFE) $(S^*, 0, 0) = (\frac{r-\mu}{\mu\delta}, 0, 0)$. To ensure that S_e, I_e and S^* are positive, we require $\mu < x < \min(r, \mu+\nu)$. We begin by showing that the density of susceptibles at the EE is lower than at the DFE.

Proposition 4. *Suppose the EE exists. Then $S_e(x) < S_e(\mu) = S^*$.*

Proof. We show that S_e is a decreasing function of x in the relevant range $\mu < x < \min(r, \mu+\nu)$. This proves the claim. Substituting (16) into (18) gives the expression

$$S_e(x) = \frac{(r-x)(\mu+\nu-x)}{\nu\delta x}. \tag{20}$$

Differentiating (20) with respect to x, we get

$$\frac{dS_e}{dx} = \frac{1}{\delta\nu}\left(1 - \frac{(\mu+\nu)r}{x^2}\right).$$

The term in brackets is negative as long as $x < \min(r, \mu+\nu)$. □

While the calculations were for general transmission terms up to now, we have to consider a special case form here on because the logarithmic terms lead to transcendental equations for the equilibrium, so that no explicit solution is available. Therefore, we make the assumption that aggregation is low, i.e. we consider the case $k_d, k_e \to \infty$. Then using Remark 1, we replace model (6) with

$$\begin{aligned}
\frac{dS}{dt} &= \frac{r(S+(1-\alpha)I)}{1+\delta N} - \mu S - S\frac{\lambda_d(N)p_d I}{N} - S\frac{\lambda_e p_e V}{1+\sigma V} \\
\frac{dI}{dt} &= \frac{\alpha r I}{1+\delta N} - (\mu+\nu)I + S\frac{\lambda_d(N)p_d I}{N} + S\frac{\lambda_e p_e V}{1+\sigma V} \\
\frac{dV}{dt} &= -\tau V + \epsilon I
\end{aligned} \tag{21}$$

Setting the right hand side of the second equation of (21) to zero, inserting the explicit expressions for $S_e, I_e, V_e > 0$ and rewriting in terms of x, we obtain

$L(x) = 0$, where

$$L(x) = \alpha x - (\mu + \nu) + \lambda_d(N_e)p_d\frac{\mu + \nu - x}{\nu} + \frac{\lambda_e p_e \varepsilon(r - x)(\mu + \nu - x)}{\sigma\varepsilon(x - \mu)(r - x) + \delta\tau\nu x}. \tag{22}$$

Thus, finding an EE for system (21) reduces to solving $L(x) = 0$ in the interval $\mu < x < \min(r, \mu + \nu)$. The following lemma connects the properties of $L(x)$ with stability of the DFE and gives a partial answer for the existence of an EE.

Lemma 4.1. *(a) The DFE of (21) is unstable if and only if $L(\mu) > 0$.*
(b) If the DFE is unstable, $r > \mu + \nu$, and $\alpha < 1$, then there is at least one EE of (21).
(c) If the DFE is unstable, $r < \mu + \nu$, and $r\left(\alpha - \frac{\lambda_d p_d}{\nu}\right) + (\mu + \nu)\left(\frac{\lambda_d p_d}{\nu} - 1\right) < 0$, then there is at least one EE of (21).

Proof. (a) Substituting $x = \mu$ into $L(x) > 0$ and solving for r gives exactly the reverse inequality of (15).
(b) If $r > \mu + \nu$ and $\alpha < 1$, then L is a continuous function for $\mu \le x \le \mu + \nu$. Furthermore,

$$L(\mu + \nu) = (\alpha - 1)(\mu + \nu) \le 0.$$

Since $\alpha < 1$, L has a sign change in the interval $(\mu, \mu + \nu)$ and therefore also a zero.

The proof of (c) follows from the fact the third condition is equivalent to $L(r) < 0$, which implies that $L(x)$ changes sign on (μ, r). □

To get a complete answer about existence and uniqueness of the EE in terms of parameters, we consider the special case that λ_d is a constant, independent of N, i.e. we consider the case of frequency-dependent transmission rate. Then $L(x) = 0$ can be written as $C(x) = 0$, where $C(x) = a_3x^3 + a_2x^2 + a_1x + a_0$ is a cubic polynomial with coefficients

$$a_3 = \sigma\frac{\varepsilon}{\nu}(\lambda_d p_d - \alpha\nu),$$

$$a_2 = \sigma\varepsilon(\mu + \nu) + \alpha(\sigma\varepsilon(r + \mu) + \delta\tau\nu) - \frac{1}{\nu}\lambda_d p_d(\sigma(2\mu + \nu + r)\varepsilon + \delta\tau\nu) + \lambda_e p_e\varepsilon,$$

$$a_1 = -(\mu + \nu)(\sigma\varepsilon(r + \mu) + \delta\tau\nu) - \alpha\sigma\varepsilon r\mu + \frac{\mu + \nu}{\nu}(\sigma(r + \mu)\lambda_d p_d\varepsilon - \lambda_e p_e\varepsilon\nu + \lambda_d p_d\delta\tau\nu)$$
$$-\frac{r\varepsilon}{\nu}(\lambda_e p_e\nu - \sigma\lambda_d p_d\mu),$$

$$a_0 = \frac{(\mu + \nu)r\varepsilon}{\nu}(\sigma\mu\nu + \lambda_e p_e\nu - \sigma\mu\lambda_d p_d).$$

We define $\hat{\mu} = \min(r, \mu + \nu)$. The following proposition gives a sufficient condition for existence and uniqueness of EE.

Proposition 5. *Suppose $C(\mu) > 0$, $C(\hat{\mu}) < 0$, and either*
(a) $a_3 > 0$
or
(b) $a_3 < 0$ and either $C''(\mu) \le 0$ or $C''(\hat{\mu}) \ge 0$.
Then $C(x)$ has exactly one zero in the interval $(\mu, \hat{\mu})$.

Proof. Existence of such a zero follows from the Intermediate Value Theorem.

If (a) holds, then $C(x) \to \infty$ as $x \to \infty$, and $C(x) \to -\infty$ as $x \to -\infty$. Then, again by the Intermediate Value Theorem, $C(x)$ has at least one zero in $(-\infty, \mu)$ and at least one zero in $(\hat{\mu}, \infty)$. Since $C(x)$ is a cubic polynomial, it has exactly one root in $(\mu, \hat{\mu})$ (see Figure 1).

Suppose (b) holds. Then $C''(x) = 6a_3x + 2a_2$ is a decreasing linear function. If $C''(\mu) \leq 0$, then $C(x)$ is concave down throughout the interval $(\mu, \min(r, \mu+\nu))$. If $C''(\hat{\mu}) \geq 0$, then $C(x)$ is concave up throughout the interval $(\mu, \min(r, \mu+\nu))$. In both cases, $C(x)$ has exactly one zero in the interval $(\mu, \min(r, \mu+\nu))$ (see Figure 1). □

Remark 3. In the non-generic case $a_3 = 0$, the same argument as in (a) carries through for the quadratic polynomial $C(x)$. Depending on the sign of a_2, there will be a second zero either in $(-\infty, \mu)$ or in $(\hat{\mu}, \infty)$. If, in addition, $a_2 = 0$, we get a linear function with a single zero.

We want to express the sufficient conditions for existence and uniqueness of the EE in terms of model parameters. If $a_3 < 0$ then the conditions $C''(\mu) \leq 0$, $C''(\mu+\nu) \geq 0$ and $C''(r) \geq 0$ are equivalent to

$$r\sigma \leq \frac{\varepsilon\mu\nu(2\alpha-1) - \nu^2(\sigma\varepsilon + \alpha\delta\tau) + \lambda_d p_d(\sigma\varepsilon(\nu-\mu) + \delta\tau\nu) - \lambda_e p_e \varepsilon\nu}{\varepsilon(\alpha\nu - \lambda_d p_d)}, \tag{23}$$

$$r\sigma \geq \frac{\sigma\varepsilon\mu\nu(2\alpha-1) - \nu^2(\sigma\varepsilon + \alpha\delta\tau - 3\varepsilon\alpha) + \lambda_d p_d(\delta\tau\nu - \sigma\varepsilon(\mu+2\nu)) - \lambda_e p_e \varepsilon\nu}{\varepsilon(\alpha\nu - \lambda_d p_d)}, \tag{24}$$

$$r\sigma \leq \frac{\nu(\sigma\varepsilon((1+\alpha)\mu+\nu) + \lambda_e p_e) + \alpha\nu\delta\tau - \lambda_d p_d((2\mu+\nu)\sigma\varepsilon + \delta\tau\nu)}{2\varepsilon(\alpha\nu - \lambda_d p_d)}, \tag{25}$$

respectively.

Using Remark 2 and Lemma 4.1 (recalling that λ_d is constant), we see that the condition $C(\mu) > 0$ is equivalent to

$$r > \mu + \frac{\delta\tau\mu}{\lambda_e p_e \varepsilon}((\mu+\nu) - \alpha\mu - \lambda_d p_d). \tag{26}$$

Finally, the conditions $C(\mu+\nu) < 0$ (used in the case when $r > \mu+\nu$) and $C(r) < 0$ (used when $r < \mu+\nu$) can be shown to be equivalent to

$$r\sigma > (\mu+\nu)\left(\sigma - \frac{\delta\tau}{\varepsilon}\right), \tag{27}$$

and

$$r(\alpha\nu\tau - \lambda_e p_e \varepsilon) > (\mu+\nu)(\nu\tau - \lambda_e p_e \varepsilon), \tag{28}$$

respectively. Note that if $r > \mu+\nu$, then condition (27) always holds, and thus so does $C(\mu+\nu) < 0$ (see also Lemma 4.1).

Summarizing the above observations, we obtain the following sufficient condition for existence and uniqueness of the EE of (21).

Corollary 1. *Assume that (26) is satisfied. Then we have the following sufficient conditions for the existence and uniqueness of the EE.*
1) If $r > \mu+\nu$: Either $\lambda_d p_d > \alpha\nu$ or (23) or (24) hold.
2) If $r < \mu+\nu$: Inequality (28) holds and either $\lambda_d p_d > \alpha\nu$ or (23) or (25) hold.

5. **Bifurcation analysis of DFE and EE.** In this section, we investigate the question of the emergence of an EE in the general model (6) using center manifold theory. We show that, under a mild technical assumption, a forward bifurcation occurs at $R_0 = 1$. In particular, $R_0 = 1$ is the threshold for disease control. The advantage of this approach over the direct approach in the previous section is that we obtain our result for all values of k_d, k_e. The disadvantage is that it only considers values of R_0 close to one. We choose the unspecific harvesting parameter μ as our

bifurcation parameter, since this is the only quantity that humans can reasonably control. We assume that λ_d is constant.

First, note that $R_0 < 1$ is equivalent to

$$(1-\alpha)\mu^2 + \left(\nu - \lambda_d p_d + \frac{\lambda_e p_e \varepsilon}{\delta\tau}\right)\mu - \frac{r\lambda_e p_e \varepsilon}{\delta\tau} > 0.$$

If $\alpha = 1$ and $\nu - \lambda_d p_d + \frac{\lambda_e p_e \varepsilon}{\delta\tau} \le 0$, then $R_0 > 1$ for any value of $\mu > 0$. Thus, we can assume that $\alpha < 1$ or $\nu - \lambda_d p_d + \frac{\lambda_e p_e \varepsilon}{\delta\tau} > 0$. In this case, define μ_{cr} to be the positive root of

$$(1-\alpha)\mu^2 + \left(\nu - \lambda_d p_d + \frac{\lambda_e p_e \varepsilon}{\delta\tau}\right)\mu - \frac{r\lambda_e p_e \varepsilon}{\delta\tau} = 0.$$

Then $R_0 < 1$ is equivalent to $\mu > \mu_{cr}$.

We state the main theorem here; the rest of this section is devoted to the proof.

Theorem 5.1. *Suppose that*

$$\tau^2\alpha\delta\mu^2\nu - \tau\epsilon\lambda_e p_e(r(\mu+\nu) - \mu^2) -$$
$$\mu^2\delta S^*\tau^2\lambda_d p_d\left(\frac{1}{S^*} + \frac{\lambda_d p_d}{2k_d}\right) - \mu^2\delta(S^*)^2\epsilon^2\lambda_e p_e\left(\sigma + \frac{\lambda_e p_e}{2k_e}\right) < 0. \tag{29}$$

Then for $\mu < \mu_{cr}$ with $|\mu - \mu_{cr}|$ small, the DFE $(S^*, 0, 0)$ is unstable, and there is a locally stable endemic equilibrium (S^{**}, I^{**}, V^{**}). Moreover, $0 < S^{**} < S^*$, and $I^{**}, V^{**} > 0$. For $\mu > \mu_{cr}$ with $|\mu - \mu_{cr}|$ small, the DFE is locally asymptotically stable.

Corollary 2. *For sufficiently small $\alpha, \tau > 0$, the condition (5.1) is satisfied, and thus, there is no backward bifurcation with respect to μ.*

Proof. Follows from continuity of the expression (5.1) and the fact that for $\tau = \alpha = 0$ the condition is satisfied (note that the term $r(\mu+\nu) - \mu^2$ is positive by our assumption that $r > \mu$). □

The above corollary motivates us to conjecture that R_0 is the actual disease eradication threshold. Numerical simulations seem to support this conjecture.

The proof of this theorem relies on an application of the Theorem 7.1 from Appendix A.

We formulate our model (6) as $\frac{d\mathbf{x}}{dt} = \mathbf{f}(\mathbf{x}; \mu)$, where $\mathbf{x} = (S, I, V)^T$, $\phi = \mu$, and $\mathbf{f} = (f_1, f_2, f_3)^T$ is the right hand side of (6). The DFE is the equilibrium $(x_1^*(\mu), x_2^*(\mu), x_3^*(\mu))^T$ where

$$x_1^*(\mu) = S^*(\mu) = \frac{r-\mu}{\delta\mu}, \quad x_2^*(\mu) = 0, \quad x_3^*(\mu) = 0.$$

The Jacobi matrix J is given by (8). When $\mu = \mu_{cr}$, matrix J has a simple zero eigenvalue. The other two eigenvalues are negative: one is given by the entry $(J)_{11} = -\frac{\mu^2\delta S^*}{r}$, and the other is the trace of its minor,

$$\operatorname{tr}(M_{11}) = -(1-\alpha)\mu - \nu + \lambda_d(S^*)p_d - \tau = -\frac{S^*\lambda_e p_e \varepsilon}{\tau} - \tau < 0,$$

since for $\mu = \mu_{cr}$ inequality (10) is an equality.

The left and right eigenvector corresponding to the zero eigenvalue of J are $\mathbf{v} = (v_1, v_2, v_3) = (0, \tau, S^*\lambda_e p_e)$ and

$$\mathbf{w} = (w_1, w_2, w_3) = \left(\frac{\tau}{r}(\mu^2 - r(\mu+\nu)), \frac{\mu^2\delta S^*\tau}{r}, \frac{\mu^2\delta S^*\varepsilon}{r}\right),$$

respectively. Note that $\mathbf{w}\cdot\mathbf{v} > 0$, $w_1 < 0$ (since $S^* > 0$ implies $r > \mu$), and $w_2, w_3 > 0$.

We need to calculate the signs of

$$a = \frac{1}{2}\sum_{i,j,k=1}^{3} v_i w_j w_k \frac{\partial^2 f_i}{\partial x_j \partial x_k}(x^*, \mu),$$

and

$$b = \sum_{k,i=1}^{3} v_k w_i \left(\sum_{j=1}^{3} \frac{\partial^2 f_k}{\partial x_i \partial x_j}(\mathbf{x}^*; \mu)\frac{dx_j^*}{d\mu} + \frac{\partial^2 f_k}{\partial x_i \partial \mu}(\mathbf{x}^*; \mu) \right),$$

both evaluated at $\mu = \mu_{\rm cr}$.

Since $v_1 = 0$, all terms with second derivatives of f_1 vanish from the expression for a and b. Furthermore, since $f_3(S, I, V) = -\tau V + \varepsilon I$ is linear, its second derivatives also vanish. Finally, since $I^* = x_2^* = 0$ and $V^* = x_3^* = 0$ are independent of μ, the terms that contain these derivatives vanish as well. With these simplifications, the expressions for a and b reduce to

$$a = \frac{1}{2}v_2\left(w_1^2\frac{\partial f_2}{\partial S^2} + 2w_1w_2\frac{\partial f_2}{\partial S\partial I} + 2w_1w_3\frac{\partial f_2}{\partial S\partial V} + w_2^2\frac{\partial f_2}{\partial I^2} + 2w_2w_3\frac{\partial f_2}{\partial I\partial V} + w_3^2\frac{\partial f_2}{\partial V^2}\right)$$

and

$$\begin{aligned}\frac{b}{v_2} = {} & w_1\left(\frac{\partial^2 f_2}{\partial S^2}(S^*(\mu_{cr}),0,0;\mu_{cr})\frac{dS^*}{d\mu}|_{\mu=\mu_{cr}} + \frac{\partial^2 f_2}{\partial S\partial\mu}(S^*(\mu_{cr}),0,0;\mu_{cr})\right)\\ & + w_2\left(\frac{\partial^2 f_2}{\partial I\partial S}(S^*(\mu_{cr}),0,0;\mu_{cr})\frac{dS^*}{d\mu}|_{\mu=\mu_{cr}} + \frac{\partial^2 f_2}{\partial I\partial\mu}(S^*(\mu_{cr}),0,0;\mu_{cr})\right)\\ & + w_3\left(\frac{\partial^2 f_2}{\partial V\partial S}(S^*(\mu_{cr}),0,0;\mu_{cr})\frac{dS^*}{d\mu}|_{\mu=\mu_{cr}} + \frac{\partial^2 f_2}{\partial V\partial\mu}(S^*(\mu_{cr}),0,0;\mu_{cr})\right).\end{aligned}$$

The following two tables give the second derivatives of f_1 and f_2 at $(S^*, 0, 0)$. The second derivatives of f_3 are all equal to zero.

f_1	$\frac{\partial}{\partial S}$	$\frac{\partial}{\partial I}$	$\frac{\partial}{\partial V}$
$\frac{\partial}{\partial S}$	$-\frac{2\delta r}{(1+\delta S^*)^3}$	$\frac{r(\alpha\delta(1+\delta S^*)-2\delta r}{(1+\delta S^*)^3}$	$-\lambda_e p_e$
$\frac{\partial}{\partial I}$	$\frac{r(\alpha\delta(1+\delta S^*)-2\delta r}{(1+\delta S^*)^3}$	$-\frac{2\delta r(1-\alpha-\alpha\delta S^*)}{(1+\delta S^*)^3} + \frac{\lambda_d p_d(2k_d+\lambda_d p_d)}{k_d S^*}$	0
$\frac{\partial}{\partial V}$	$-\lambda_e p_e$	0	$\frac{S^*\lambda_e p_e(2k_e\sigma+\lambda_e p_e)}{k_e}$

f_2	$\frac{\partial}{\partial S}$	$\frac{\partial}{\partial I}$	$\frac{\partial}{\partial V}$
$\frac{\partial}{\partial S}$	0	$-\frac{\alpha r\delta}{(1+\delta S^*)^2}$	$\lambda_e p_e$
$\frac{\partial}{\partial I}$	$-\frac{\alpha r\delta}{(1+\delta S^*)^2}$	$-\frac{\alpha r\delta}{(1+\delta S^*)^2} - \frac{\lambda_d p_d(2k_d+\lambda_d p_d)}{k_d S^*}$	0
$\frac{\partial}{\partial V}$	$\lambda_e p_e$	0	$-\frac{S^*\lambda_e p_e(2k_e\sigma+\lambda_e p_e)}{k_e}$

Also, we have:

$$\begin{aligned}\frac{\partial^2 f_2}{\partial S\partial\mu}(S^*(\mu_{cr}),0,0;\mu_{cr}) &= 0\\ \frac{\partial^2 f_2}{\partial V\partial\mu}(S^*(\mu_{cr}),0,0;\mu_{cr}) &= 0\\ \frac{\partial^2 f_2}{\partial I\partial\mu}(S^*(\mu_{cr}),0,0;\mu_{cr}) &= -1\end{aligned}$$

Putting these expressions into the definitions of a and b together with $\frac{dS^*}{d\mu} = -\frac{r}{\delta\mu^2}$ we calculate

$$a = \frac{2\mu^2\delta S^*}{r^2}\left[\tau^2\alpha\delta\mu^2\nu - \tau\epsilon\lambda_e p_e(r(\mu+\nu)-\mu^2) - \mu^2\delta S^*\tau^2\lambda_d p_d\left(\frac{1}{S^*}+\frac{\lambda_d p_d}{2k_d}\right) - \mu^2\delta(S^*)^2\epsilon^2\lambda_e p_e\left(\sigma+\frac{\lambda_e p_e}{2k_e}\right)\right],$$

$$\begin{aligned}\frac{b}{v_2} &= \frac{\mu^2\delta\tau S^*}{r}\left[\left(\lambda_d'(S^*)p_d - \frac{\alpha r\delta}{(1+\delta S^*)^2}\right)\left(-\frac{r}{\delta\mu^2}\right)-1\right] - S^*\lambda_e p_e\varepsilon \\ &= \frac{\mu^2\delta\tau S^*}{r}\left[-\frac{\lambda_d'(S^*)p_d r}{\delta\mu^2}+\alpha-1\right] - S^*\lambda_e p_e\varepsilon.\end{aligned}$$

Hence, since $v_2 > 0$ and $\alpha \le 1$, we conclude that b is negative. Also, by the assumption in the statement of the theorem, $a < 0$.

The rest now follows by Theorem 7.1. In particular, the fact that for $\mu < \mu_{cr}$ we have $0 < S^{**} < S^*$, and $I^{**}, V^{**} > 0$ follows from $a < 0$ and the fact that the sign of each of the components of $(S^{**} - S^*, I^{**}, V^{**})$ coincides with the sign of $\frac{-2b(\mu-\mu_{cr})}{a} w_i$ for $i = 1, 2, 3$.

6. **Numerical results.** In this section, we illustrate the results from the previous sections and explore how various quantities depend on parameter values. We begin with the contact rate $\lambda_d(N) = \bar{\lambda}_d$ that leads to a frequency-dependent direct transmission term. Among other things, we demonstrate that harvesting does reduce R_0 and hence can be used as a management strategy. We use Latin Hypercube sampling and partial rank correlation coefficients show how R_0 depends on model parameters. Next, we illustrate the effects of aggregation parameters on disease prevalence. Finally, we explore how the functional form of the contact rate affects our results.

We chose parameter values and ranges from the literature; see Table 2. The "value" is used for numerical simulation, unless otherwise noted; the "range" is used for Latin Hypercube sampling. Since the data are from different geographical locations and species, we do not claim that the chosen data represent a specific system; rather they give rough estimates for a general model.

parameter	meaning	value	range	unit	ref.
r	growth rate	1.1	0.5-1.5	$\frac{1}{t}$	[11]
μ	common death rate	0.3	0.05-0.3	$\frac{1}{t}$	[11]
α	hereditary infection factor	0.05	0.05	-	[13]
δ	logistic growth coefficient	0.05	0-0.1	$\frac{1}{\#}$	[11]
$\beta_d = \bar{\lambda}_d p_d$	"effective" direct contact rate	0.4	0.4-0.5	$\frac{1}{t}$	[23]
$\beta_e = \lambda_e p_e$	"effective" indirect contact rate	0.777	0.777-0.799	$\frac{1}{t}$	[18]
ν	death rate due to the disease	0.5	0.369-0.641	$\frac{1}{t}$	[18]
τ	prion decay rate	2.55	$2.51-2.59$	$\frac{1}{t}$	[18]
ε	prion shedding rate	0.111	0.109-0.113	$\frac{\diamondsuit}{\#t}$	[18]

TABLE 2. Parameters and their potential ranges for model simulation and Latin Hypercube sampling. We consider the limiting case $k_{d,e} \to \infty$. The contact rate is $\lambda_d(N) = \bar{\lambda}_d$, which leads to frequency-dependent transmission. We use thousands of deer as the unit #.

We assume that the prion saturation constant is given by $\sigma = 10^{-5}(\frac{1}{\diamondsuit})$. We also assume that additional harvesting varies from 0 to 0.7.

Remark 4. Based on numerics, we observe that for the chosen parameter ranges, the inequality (5.1) always holds (i.e. $a < 0$), and, thus, Theorem 5.1 applies in our case.

Without harvesting ($\mu = 0.3$), we calculate $R_0 = 2.7736$. The DFE is unstable for the chosen parameter values; solutions converge to the EE (Figures 2). With sufficient harvesting ($\mu = 0.3 + 0.6 = 0.9$), we find $R_0 = 0.4252$. The DFE becomes stable and $I, V \to 0$ (Figures 3). According to Remark 2, we have the critical growth rate $r_{cr} \approx 0.4707 < r = 1.1$ in the absence of harvesting ($\mu = 0.3$) and $r_{cr} \approx 2.1706 > r = 1.1$ with harvesting ($\mu = 0.9$). In the former case, case the sufficient condition of existence of EE from Proposition 5 (a) ($a_3 > 0$) holds true. In the second case (Fig. 3), the DFE is stable. Hence, these simulations confirm the theoretical result that harvesting can be used to control the population. In simple models with frequency-dependent transmission, there is no population threshold for R_0 [15]. However, even in those models, R_0 depends on population mortality, and thereby on harvesting. In our case, the additional indirect transmission term is directly affected by population levels (and therefore by harvesting). The combination of these two effects allows us to control the disease by harvesting.

We illustrate the dependence of R_0 on parameters by calculating partial rank correlation coefficients (PRCCs) with the use of Latin Hypercube sampling as well as the elasticity (Figures 4). The intervals from which parameter values are chosen are given in Table 2. The strength of density dependence in the logistic growth function, the natural and disease-induced death rate and the prion decay rate all affect R_0 negatively. Increasing any of the first three parameters will decrease the population and thereby lower R_0. Increasing the prion decay rate will decrease the mean time for which prions are present in the environment, and thereby lower R_0. The elasticity plot shows that a significant change in the direct contact rate is needed to reduce R_0 by 1%, but only a small change in indirect contact rate is necessary for the same change.

Figure 8 illustrates dependence of R_0 on additional harvesting, with parameters given by Table 2, and additional harvesting in the range $0 - 0.7$. We observe that increasing harvesting decreases the value of R_0, with values below 1 for sufficiently high harvesting rates.

Next, we explore the dependence of the susceptible and infected populations at EE on aggregation levels $k_d, k_e < \infty$. For simplicity, we assume $k_d = k_e = k$. Figure 6 shows the fraction of the population relative to the disease-free carrying capacity and the prevalence of the disease at the EE as a function of aggregation parameter k. An increase in k leads to a decrease in total population and an increase in prevalence. We conclude that high aggregation (low k) is beneficial for the population whereas low aggregation is beneficial for the disease.

As the decay rate of prions in the environment (τ) increases, the infection risk for susceptibles from these prions decreases. We have already seen that the basic reproduction number is a decreasing function of τ (or an increasing function of the average lifetime of prions in the environment $1/\tau$). Figure 7 shows that the prevalence at steady state decreases with τ whereas the total population increases with τ.

7. **Conclusions.** Disease transmission depends on how the pathogen interacts with the social and behavioral structure of the host population. Many diseases in cervids (as well as other species) have more than one transmission pathway. Besides CWD, this is also true for bovine tuberculosis, brucellosis and other infections [7]. A crucial question in the control of such diseases is which pathway contributes most to disease transmission. We chose CWD as one example of a wildlife disease with direct and indirect (environmental) transmission. We formulated a strategic model of only three compartments to evaluate the relative importance of the different transmission pathways and the effect of behavior on prevalence.

On the theoretical side, we found some explicit conditions for the existence of an endemic equilibrium and its uniqueness. In general, we used center manifold theory to prove that this system does exhibit a forward bifurcation, with a biologically relevant stable EE appearing for $R_0 > 1$. We found parameter values for CWD in the literature and performed a sensitivity and elasticity analysis of R_0 via Latin hypercube sampling. We found that R_0 is more sensitive to the indirect than the direct contact rate, and that a much larger change in the direct contact rate is required to decrease R_0 by 1%. This finding confirms some results by Almberg and coworkers who tested the relative importance of direct and indirect transmission of CWD in a large simulation model [2]. We also confirm another result of those authors that prevalence increases with environmental life span of prions.

In terms of the disease management, we found that increase in harvesting can be used to control the spread of CWD, by reducing R_0. There are however cases when increasing μ does not help to reduce R_0: as we observed in Section 5, when $\alpha = 1$ (i.e. offspring of infected class remains infected) or $\nu - \lambda_d p_d + \frac{\lambda_e p_e \varepsilon}{\delta \tau} \leq 0$ (i.e. direct contact rate is relatively high), $R_0 > 1$ for any $\mu > 0$. Otherwise, our bifurcation result, given that R_0 is close to 1 (i.e. we are in a critical situation) suggests that increasing μ will result in disease eradication. However, confirming this conjecture will require a proof of global stability of the DFE.

Other possible control strategies aiming at reducing R_0 include creation of buffer zones to separate the animals and/or removal of animal carcasses, thus, decreasing both the direct and indirect contact rate (see also [13]).

Although we developed our model to describe a particular disease, it can be easily adapted to describe different settings, such the spread of infectious diseases in human population via both direct and indirect contact. Many infections are transmitted by direct contact as well as through surfaces, and numerous recommendations for disease control focus on indirect transmission (frequent hand washing, disinfection of surfaces).

We see a major future challenge in modeling direct and indirect disease transmission when space and spatial movement are considered explicitly. It will be particularly interesting to see whether more mechanistic models for group formation will confirm the importance of aggregation on disease prevalence.

Acknowledgments. This work was supported by a PrioNet Canada grant. We are grateful for discussions with Margit Westphal and Prof. Daniel Krewski (University of Ottawa).

Appendix A. A technical theorem used in bifurcation analysis. Here we include a result used in Section 5.

Theorem 7.1 (c.f. Theorem 4.1 in [5]). *Consider a system of ODE's with a parameter ϕ:*

$$\frac{d\mathbf{x}}{dt} = \mathbf{f}(\mathbf{x};\phi), \quad \mathbf{f}:\mathbb{R}^3\times\mathbb{R}\to\mathbb{R}^3, \quad \mathbf{f}\in C^2(\mathbb{R}^3\times\mathbb{R}).$$

Assume $\mathbf{x}^*(\phi) = (x_1^*(\phi), x_2^*(\phi), x_3^*(\phi))^T$ is a steady state for all ϕ and $x_1^*(\phi) > 0$. Denote by $J = D_{\mathbf{x}}\mathbf{f}(\mathbf{x}^*(\phi_0);\phi_0)$ the Jacobi matrix at $\mathbf{x}^*(\phi_0)$. Assume that 0 is a simple eigenvalue of J, and the other eigenvalues of J have negative real parts.

Denote $\mathbf{w}, \mathbf{v}$ as the right and left eigenvectors corresponding to the zero eigenvalue of J, and assume $\mathbf{w}\cdot\mathbf{v} > 0$.

Denote by f_k be the kth component of $\mathbf{f}$, and define the two quantities

$$a = \sum_{k,i,j=1}^{3} v_k w_i w_j \frac{\partial^2 f_k}{\partial x_i \partial x_j}(\mathbf{x}^*(\phi_0);\phi_0),$$

and

$$b = \sum_{k,i=1}^{3} v_k w_i \left(\sum_{j=1}^{3} \frac{\partial^2 f_k}{\partial x_i \partial x_j}(\mathbf{x}^*(\phi_0);\phi_0)\frac{dx_j^*}{d\phi}|_{\phi=\phi_0} + \frac{\partial^2 f_k}{\partial x_i \partial \phi}(\mathbf{x}^*(\phi_0);\phi_0) \right).$$

Then the local dynamics of the system near $(\mathbf{x}^*, \phi_0)$ are fully determined by the signs of a and b as described below.

1. *$b > 0$. When $\phi < \phi_0$ with $|\phi - \phi_0| \ll 1$, $\mathbf{x}^*(\phi)$ is locally asymptotically stable, and there exists an unstable equilibrium $\mathbf{x}^{**}(\phi)$; when $\phi > \phi_0$ with $|\phi - \phi_0| \ll 1$, $\mathbf{x}^*(\phi)$ is unstable, and there exists a locally asymptotically stable equilibrium $\mathbf{x}^{**}(\phi)$;*
2. *$b < 0$. When $\phi < \phi_0$ with $|\phi - \phi_0| \ll 1$, $\mathbf{x}^*(\phi)$ is unstable, and there exists a locally stable equilibrium $\mathbf{x}^{**}(\phi)$; when $\phi > \phi_0$ with $|\phi - \phi_0| \ll 1$, $\mathbf{x}^*(\phi)$ is locally asymptotically stable, and there exists an unstable equilibrium $\mathbf{x}^{**}(\phi)$;*

In both cases, the sign of $x_i^{**}(\phi) - x_i^*(\phi)$ coincides with the sign of $\frac{-2b(\phi-\phi_0)}{a} w_i$.

This theorem follows from Theorem 4.1 of [5] by the change of variables $\tilde{\mathbf{x}} = \mathbf{x} - \mathbf{x}^*(\phi)$, $\tilde{\phi} = \phi - \phi_0$, and

$$\frac{d\tilde{\mathbf{x}}}{dt} = \tilde{\mathbf{f}}(\tilde{\mathbf{x}}, \tilde{\phi}) = \mathbf{f}(\tilde{\mathbf{x}} + \mathbf{x}^*(\phi' + \phi_0), \phi' + \phi_0).$$

and applying the chain rule of differentiation.

8. Figures

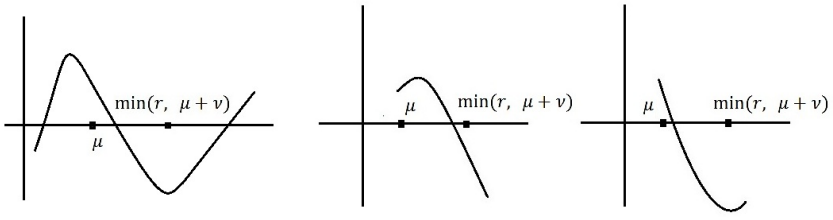

FIGURE 1. Illustration of the proof of Proposition 5. Left plot: case (a) ($a_3 > 0$) right plot; case (b) ($a_3 < 0$), middle and right plot.

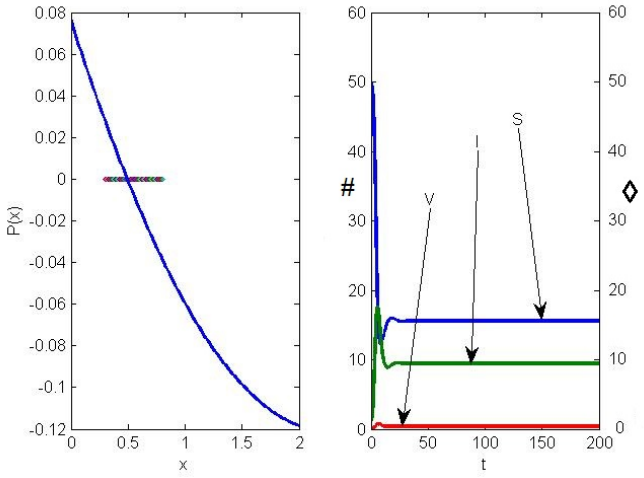

FIGURE 2. Graph of the polynomial $P(x)$ (left) and the corresponding solution curves (right) when $R_0 = 2.8075 > 1$ so that the DFE is unstable and solutions approach the EE. The highlighted interval on the graph of $P(x)$ is $[\mu, \hat{\mu}] = [\mu, \mu+\nu] = [0.3, 0.8]$. Note that $P(\mu) > 0$ and $P(\mu+\nu) < 0$, with the root of $P(x)$ corresponding to the EE. Parameter values are $\mu = 0.3$ and otherwise as in Table 2. We use thousands of deer as the unit for S and I.

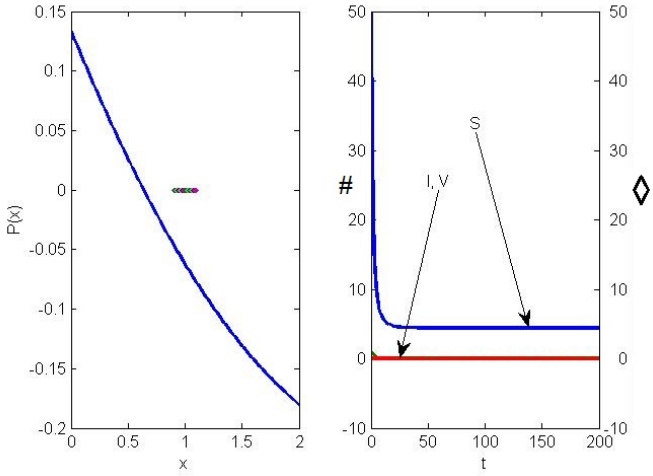

FIGURE 3. Graph of the polynomial $P(x)$ (left) and the corresponding solution curves (right) when $R_0 = 0.4061 < 1$, so that the DFE is stable. The highlighted interval on the graph of $P(x)$ is $[\mu, \hat{\mu}] = [\mu, r] = [0.9, 1.1]$. Note that $P(x) < 0$ throughout the highlighted interval. Parameter values are $\mu = 0.9$ and otherwise as in Table 2. We use thousands of deer as the unit for S and I.

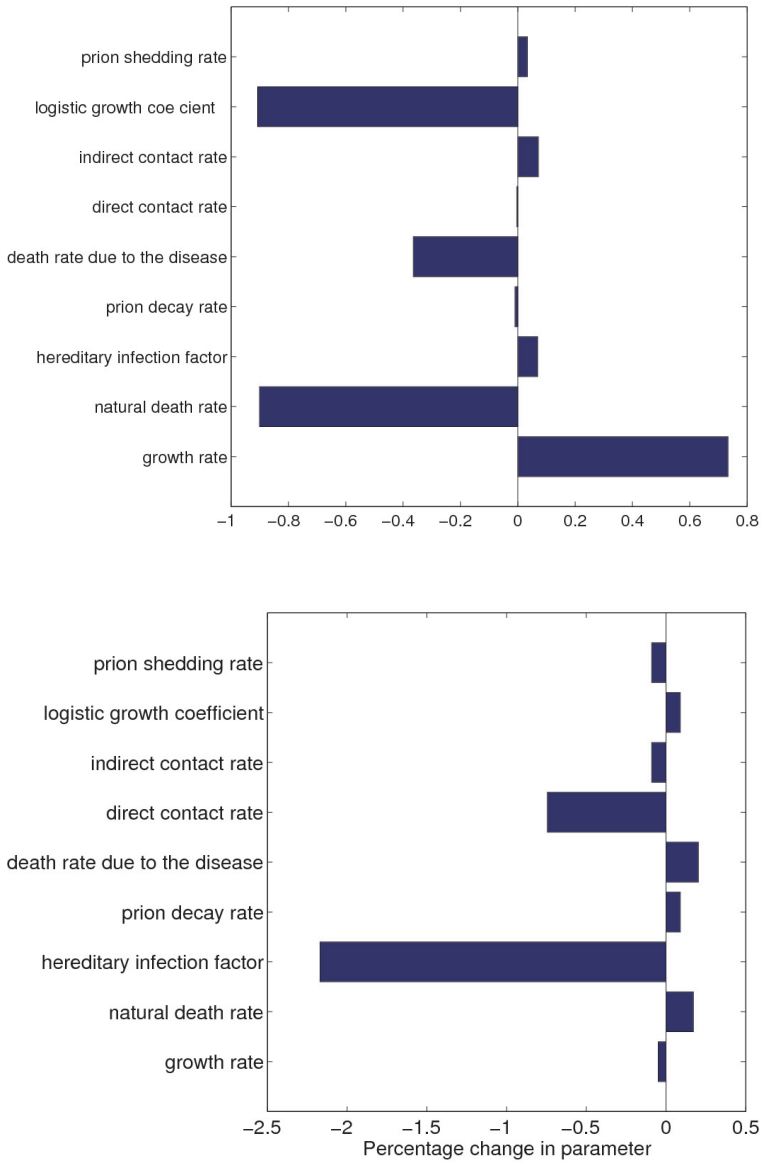

FIGURE 4. Tornado graph for the partial rank correlation coefficients (top panel) and the elasiticity (bottom panel, using logarithmic scale) of R_0 with respect to model parameters. The elasticity indicates the percentage change required in the parameter to obtain a 1% decrease in R_0.

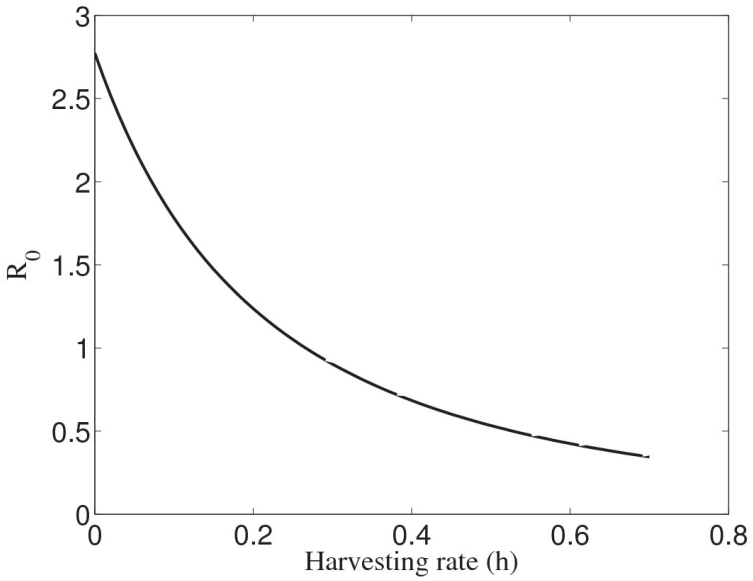

FIGURE 5. Dependence of R_0 on additional harvesting rate h, taking values from 0 to 0.7. Here the natural death rate is given by $\mu = 0.3$ (which combined with h is varying in the range of $0.3 - 1$), and other parameters are as in Table 2.

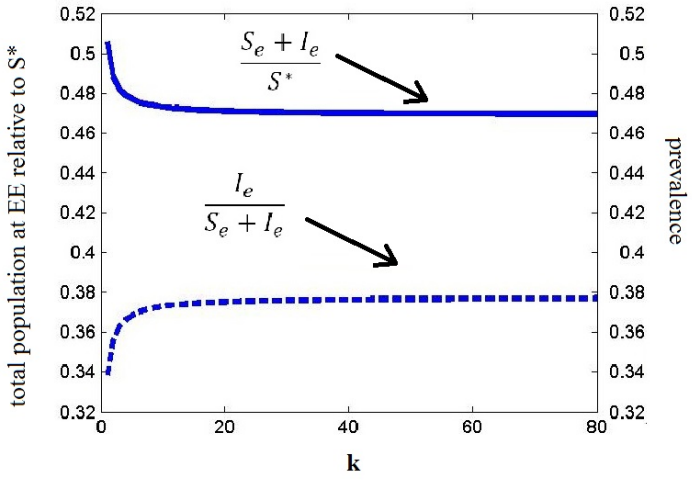

FIGURE 6. Dependence of the total population and prevalence at endemic equilibrium on aggregation $k_d = k_e = k$. Here $\mu = 0.3$ and other parameters are as in Table 2.

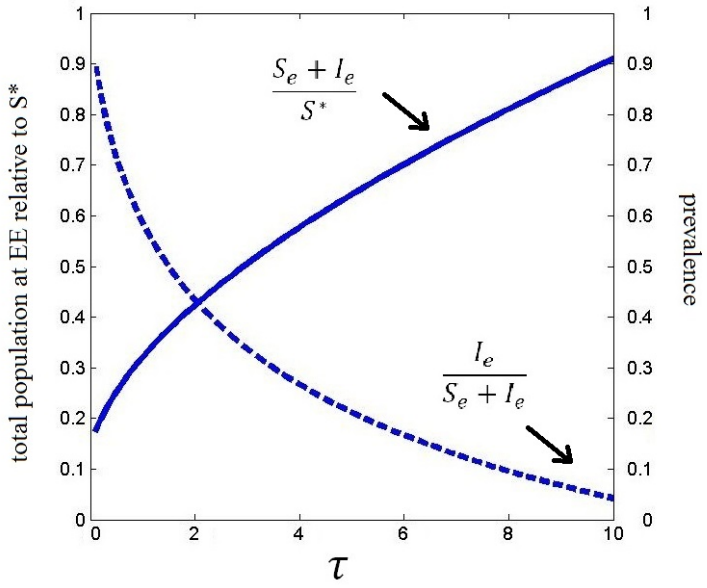

FIGURE 7. Dependence of the total population and prevalence at endemic equilibrium on prion decay rate. Here $\mu = 0.3$ and other parameters are as in Table 2.

REFERENCES

[1] A. Aguzzi, M. Heikenwalder and M. Polymenidou, Insights into prion strains and neurotoxicity, *Nature Reviews Molecular Cell Biology*, **8** (2007), 552–561.

[2] E. Almberg, P. Cross, C. Johnson, D. Heisey and B. Richards, Modeling routes of Chronic Wasting Disease transmission: Environmental prion persistence promotes deer population decline and extinction, *PLoS One*, **6** (2011), e19896.

[3] M. Begon, M. Bennett, R. G. Bowers, N. P. French, S. M. Hazel and J. Turner, A clarification of transmission terms in host-microparasite models: Numbers, densities and areas, *Epidemiology* and *Infection*, **129** (2002), 147–153.

[4] R. Breban, Role of environmental persistence in pathogen transmission: A mathematical modeling approach, *J. Math. Biol.*, **66** (2013), 535–546.

[5] C. Castillo-Chavez and B. Song, Dynamical models of tuberculosis and their applications, *Mathematical Biosciences and Engineering*, **1** (2004), 361–404.

[6] J. Collinge and A. R. Clarke, A general model of prion strains and their pathogenicity, *Science*, **318** (2007), 930–936.

[7] M. M. Conner, M. R. Ebinger, J. A. Blanchong and P. C. Cross, Infectios disease in cervids of North America, *Ann. N.Y. Acad. Sci.*, **1134** (2008), 146–172.

[8] 2.0.CO;2] M. M. Conner, M. W. Miller, M. R. Ebinger and K. P. Burnham, A meta-BACI approach for evaluating management intervention on chronic wasting disease in mule deer, *Ecological Applications*, **17** (2007), 140–153.

[9] O. Diekmann and J. A. M. Heesterbeek, *Mathematical Epidemiology of Infectious Diseases: Model Building, Analysis and Interpretation*, John Wiley & Sons, 2000.

[10] K. Dietz, Overall population patterns in the transmission cycle of infectious disease agents, *Population Biology of Infectious Diseases, ed. R.M. Anderson and R.M. May, Dahlem Konferenzen, Springer-Verlag*, **25** (1982), 87–102.

[11] G. L. Dusek, R. J. MacKie, J. D. Herriges and B. B. Compton, Population ecology of white-tailed deer along the Lower Yellowstone River, *Wildlife Monographs*, **104** (1989), 3–68.

[12] H. R. Fryer and A. R. McLean, There is no safe dose of prions, *PLoS ONE*, **6** (2011), e23664.

[13] J. E. Gross and M. W. Miller, Chronic wasting disease in mule deer: Disease dynamics and control, *The Journal of Wildlife Management*, **65** (2001), 205–215.
[14] T. Habib, E. Merrill, M. J. Pybus and D. Coltman, Modelling landscape effects on density-contact rate relationships in eastern Alberta: Inplications for chronic wasting disease, *Ecological Modelling*, **222** (2011), 2722–2732.
[15] J. O. Lloyd-Smith, P. C. Cross, C. J. Briggs, M. Daugherty, W. M. Getz, J. Latto, M. S. Sanchez, A. B. Smith and A. Swei, Should we expect population thresholds for wildlife disease?, *Trends in Ecology & Evolution*, **20** (2005), 511–519.
[16] C. K. Mathiason, S. A. Hays, J. Powers, J. Hayes-Klug and J. Langenberg, et al, Infectious prions in pre-clinical deer and transmission of chronic wasting disease solely by environmental exposure, *PLoS ONE*, **4** (2009), e5916.
[17] R. M. May, Host-parasitoid systems in patchy environments: A phenomenological model, *Journal of Animal Ecology*, **47** (1978), 833–844.
[18] M. W. Miller, N. T. Hobbs and S. J. Tavener, Dynamics of prion disease transmission in mule deer, *Ecological Applications*, **16** (2006), 2208–2214.
[19] M. W. Miller, E. S. Williams, N. T. Hobbs and L. L. Wolfe, Environmental sources of prion transmission in mule deer, *Emerg. Infect. Dis.*, **10** (2004), 1003–1006.
[20] P. R. Moorcroft and M. A. Lewis, *Mechanistic Home Range Analysis*, Princeton University Press, 2006.
[21] E. M. Schauber and A. Woolf, Chronic wasting disease in deer and elk: A critique of current models and their application, *Wildlife Society Bulletin*, **31** (2003), 610–616.
[22] H. R. Thieme, *Mathematics in Population Biology*, Princeton Series in Theoretical and Computational Biology, Princeton University Press, 2003.
[23] G. Wasserberg, E. E. Osnas, R. E. Rolley and M. D. Samuel, Host culling as an adaptive management tool for chronic wasting disease in white-tailed deer: A modelling study, *Journal of Applied Ecology*, **46** (2009), 457–466.
[24] E. S. Williams and M. W. Miller, Chronic wasting disease in deer and elk in North America, *Revue Scientifique et technique de l'Office International des Epizzoties*, **21** (2002), 305–316.

Received March 16, 2013; Accepted October 11, 2014.

E-mail address: olga.vasilyeva@cnu.edu
E-mail address: orabytf@utpa.edu
E-mail address: flutsche@uottawa.ca